UNIVERSITY OF LEEDS

Article:
Fisher, BJ orcid.org/0000-0001-7113-2818, Moore, OW, Faust, JC et al. (2 more authors) (2020) Experimental evaluation of the extractability of Fe-bound organic carbon in sediments as a function of carboxyl content. Chemical Geology. 119853. p. 119853. ISSN 0009-2541

https://doi.org/10.1016/j.chemgeo.2020.119853

Experimental evaluation of the extractability of Fe-bound organic carbon in sediments as a function of carboxyl content.

Ben J. Fisher*, Oliver W. Moore, Johan C. Faust, Caroline L. Peacock, Christian März
School of Earth and Environment, University of Leeds, Leeds, LS2 9JT, UK

*Corresponding author (Ben.Fisher@ed.ac.uk)

Keywords:

Iron-bound organic carbon; Carboxyl group bonding; Dithionite reduction; Marine sediments; Ferrihydrite

Highlights:

- The CBD method can underestimate organic carbon bound to reactive iron in sediments
- Some organic-ferrihydrite complexes are incompletely reduced by Na dithionite at pH 7
- Some organic-ferrihydrite complexes are removable by the NaCl wash in the CBD method
- Carboxyl content of OM bound to iron affects its reactivity towards CBD reduction

Abstract:

The majority of organic carbon (OC) burial in marine sediments occurs on continental shelves, of which an estimated 10-20% is associated with reactive iron (Fe_R). The association of OC with Fe_R (OC-Fe_R) is thought to facilitate preservation of organic matter (OM) in sediments and therefore represents an important carbon sink. The citrate-bicarbonate-dithionite (CBD) method is used to quantify OC-Fe_R in marine sediments by reductively dissolving Fe_R, thereby releasing bound OC. While the CBD method is widely used, it may be less efficient at measuring OC-Fe_R than currently thought, due to the incomplete reduction of Fe_R, resulting from the neutral pH conditions required to prevent OM hydrolysis. Additionally, the typical range of values reported for OC-Fe_R in marine sediments is narrow, despite variation in OM and Fe_R inputs, OM source types and chemical compositions. This suggests a limitation exists on the amount of OC that can become associated with Fe_R, and/or that the CBD method is limited in the OC-Fe_R that it is able to quantify. In assessing the efficiency of the CBD

method, we aimed to understand whether methodological errors or (mis)interpretation of these extraction results may contribute to the apparent limitation on OC-Fe_R values. Here, we synthesised OC-Fe_R composites with a known Fe_R phase and known OM moieties, varying in carboxyl content, at neutral pH. These were spiked into OC-free marine sediment, and subject to a CBD extraction to investigate i) the efficiency of CBD for OC extraction; ii) the efficiency of CBD for Fe_R extraction; ii) how the OC moiety affects the physical parameters of associated Fe_R minerals; and iii) the impact of OM moiety on OC and Fe release. We show that the CBD method results in only partial dissolution of the most susceptible Fe_R phase (ferrihydrite) and therefore incomplete removal of bound OC. While as little as ~20% of Fe is released from OC-free ferrihydrite, structural disorder of the mineral phase increases with the inclusion of more OC, resulting in greater losses of up to 62% Fe for carboxyl rich OC-Fe_R complexes. In addition, our results show that the NaCl control step performed in the CBD method is capable of removing weakly bound OC from Fe_R, such that inclusion of this OC in the total OC-Fe_R fraction may increase marine sediments OC-Fe_R estimates by ~33%. Finally, we suggest that the structure of OC involved in OC-Fe_R binding can affect quantification of the OC-Fe_R pool. Our results have important implications for assessing the Fe_R bound OC fraction in marine sediments and the fate of this OC in the global carbon cycle.

1. Introduction

Marine sediments represent the largest organic carbon (OC) sink on Earth (Hedges and Keil, 1995) and therefore play a crucial role in the regulation of atmospheric oxygen (O_2) and carbon dioxide (CO_2) over geological time (Berner, 1989). Despite the importance of OC burial however (Burdige, 2007; Canfield, 1994), the factors that control OC burial and preservation in marine sediments are unclear (Arndt et al., 2013). One important mechanism for OM preservation appears to involve the association of OC with the reactive iron fraction in soils and sediments (Fe_R, operationally defined as the fraction of total iron that is extractable with sodium dithionate), with up to 40% of total soil OC (Wagai and Mayer, 2007) and 21.5±8.6% of total marine sediment

OC (Lalonde et al., 2012) bound to Fe_R. This Fe_R "rusty sink" (Lalonde et al., 2012) is assumed to protect OM from microbial degradation (Jones and Edwards, 1998), and help preserve OM in the Earth system (Lalonde et al., 2012).

The mechanisms responsible for OC-Fe_R associations are poorly understood, but might include chemical sorption, physical occlusion or a combination of both (Kaiser and Guggenberger, 2000; Lalonde et al., 2012; Mu et al., 2016; Wagai and Mayer, 2007). For chemical sorption to protect OC from microbial remineralisation over extended timescales, the mechanism of OC sorption with Fe_R must involve strong chemical bonds and a very high sorption coefficient (Henrichs, 1995). Work has demonstrated this using a ramped pyrolysis or oxidation method to observe the temperature decay profile of OC as a proxy for bond strength (Hemingway et al., 2017). Strong chemical bonds between OC and Fe_R are thought to be mediated via OM carboxyl (COOH) and mineral hydroxyl (OH) groups (Karlsson and Persson, 2010; Karlsson and Persson, 2012; Mikutta, 2011). The importance of carboxyl group bonding has been demonstrated by Fourier Transform Infrared Spectroscopy (FTIR) of ferrihydrite precipitated with dissolved organic matter (DOM) (Yang et al., 2012). Carboxyl groups are prevalent in marine DOM, as evidenced by carboxyl rich alicyclic molecules (CRAM) comprising a major component of refractory marine DOM (Hertkorn et al., 2006). Carboxyl groups are thought to facilitate binding of OM to Fe_R mineral surfaces via ligand exchange, whereby OM carboxyl groups replace hydroxyl groups on the mineral surface (Chen et al., 2014; Gu et al., 1994; Gu et al., 1995; Henneberry et al., 2012; Wagai and Mayer, 2007).

The citrate-dithionite-bicarbonate (CBD) method for evaluating the amount of OC-Fe_R in a sediment sample involves reduction of the present Fe_R phases, after which the reduced Fe then becomes dissolved in solution liberating bound OC. Despite widespread utilisation of the CBD method, previous studies have indicated that its efficiency may be less than originally described, whereby it was thought to dissolve all solid reactive iron phases.

For example, Adhikari and Yang (2015) performed the CBD protocol of Lalonde et al. (2012) on synthetic hematite-humic acid complexes and reported incomplete reduction ($\leqslant$ 50%) of Fe_R. Further, the CBD method has been criticised in the context of Fe speciation for its inability to fully dissolve crystalline Fe_R minerals in ancient rocks and potentially modern marine sediments (Raiswell et al., 1994). Thompson et al. (2019) showed that a CBD extraction performed at circumneutral pH fails to extract a large proportion of Fe_R minerals in modern sediments. While these studies have indicated that CBD treatment may be less efficient than currently understood, it is unknown as to why some OC-Fe_R complexes appear to be unextractable. By evaluating the efficiency of the CBD method for OC-Fe_R extraction we aim to understand the true extent to which OC-Fe_R can be extracted, and whether the structural composition of the associated organic compound influences the ability of CBD to successfully extract a particular OC-Fe_R complex. This may additionally further our understanding as to why only a minority of the sedimentary OC pool is found to be associated with Fe_R despite the fact that OC-Fe_R interactions are found to promote OC persistence. For example, the maximal OC-Fe_R content obtained by Lalonde et al. (2012) across their 42 global sediment samples was 41.69% (Wash. Coast 215), with a mean of 21.5±8.6%. Other studies employing the same CBD method also concur with this range (e.g., Zhao et al. (2018) (15.6±6.5%), Salvadó et al. (2015) (11 ± 5.5%). This poses a question as to why there is limited variability in the OC-Fe_R values obtained for sediments under differing environmental conditions, particularly where OC and Fe fluxes to the seafloor vary. To fully understand the fate of OM in marine sediments it is important to determine whether this apparent limitation in OC-Fe_R presence is a matter of methodological error/interpretation in the quantification of OC-Fe_R (by CBD), or an inherent feature of the OC-Fe_R interaction that requires further investigation.

To address the uncertainty in CBD extraction efficiency we coprecipitated model carboxylic acid compounds, containing either 1, 2 or 3 carboxyl groups, with ferrihydrite, which is ubiquitous in marine sediments and acts as a precursor for more stable Fe oxide phases (e.g., hematite) (Michel et

al., 2007). We then spiked OC-free natural sediment with our carboxylic acid-ferrihydrite coprecipitates and subject them to a CBD extraction. We investigate the efficiency of the CBD method for OC and Fe_R extraction and discuss the implications for evaluating OC-Fe_R and OM preservation with Fe_R in the marine system. We also comment on how the carboxyl character of the OC might have a significant influence on OC preservation in marine sediments.

2. Materials and Methods

2.1 Ferrihydrite coprecipitate synthesis

Following a modified method of Schwertmann and Cornell (2000), 2-line ferrihydrite was precipitated in the presence of either i) pentatonic acid ($C_5H_{10}O_2$); ii) hexanedioic acid ($C_6H_{10}O_4$) or iii) butane-1,2,4-tricarboxylic acid acid ($C_7H_{10}O_6$), which increase in their number of carboxyl groups from 1 to 3, respectively. A pure ferrihydrite sample containing no organic carbon was also precipitated as a control.

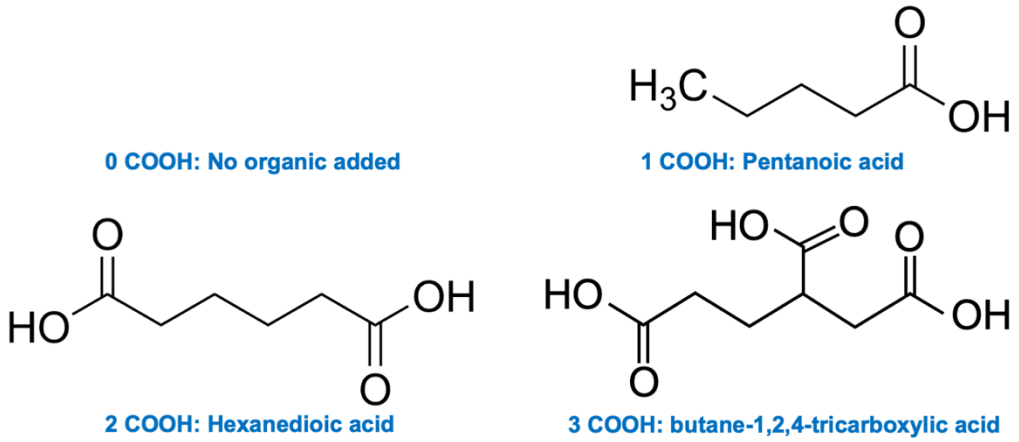

Figure 1: Chemical structures of the organic acids coprecipitated with ferrihydrite. The chemical structures of each carboxylic acid used in synthesising ferrihydrite coprecipitates are shown above their carboxyl content abbreviation (1-COOH, 2-COOH etc.) and IUPAC name. 0 COOH shows no structure as the 0 COOH coprecipitate contains no organic and instead represents a 'pure' form of ferrihydrite.

Saturation concentrations for the three organic acids were determined by increasing organic acid concentration in the mineral coprecipitation stage and measuring end state wt %C (see **Table 1)**. Saturation concentration refers to the point at which additional increases in the amount of organic

acid added did not result in a further wt% C increase in the resultant mineral coprecipitate. Coprecipitation of ferrihydrite with the named organic acids was performed by dissolving organic acids in deionised water (DI) with Fe (III) nitrate nonahydrate [$Fe(NO_3)_3.9H_2O$] (20 g/250 ml). 1 M potassium hydroxide (KOH) was then added by titration to achieve a pH of 7.0 ± 0.3.

Following coprecipitation, all of the organomineral composites were rinsed in 5L of DI water and left to gravitationally settle. This rinse step was repeated 5 times. The pentanoic acid (1-COOH) coprecipitate was rinsed three times due to slow settling of the lighter 1-COOH particles and therefore a lower yield. The pH of the resultant slurry was raised to pH 7 through dropwise addition of 0.1 M NaOH, then centrifuged (2750 g, 20 minutes) with the precipitate being retained and the supernatant discarded. Following this, the precipitate was frozen and freeze-dried. X-ray diffraction (XRD) was used to confirm the Fe mineralogy of the coprecipitate as 2-line ferrihydrite.

Table 1: Organic acids used to form ferrihydrite coprecipitates.

IUPAC Name	COOH Groups	Stoichiometry	Amount added[a]
Pentanoic acid	1	$C_5H_{10}O_2$	5 ml
Hexanedioic acid	2	$C_6H_{10}O_4$	3 g
butane-1,2,4-tricarboxylic acid	3	$C_7H_{10}O_6$	3 g

[a] values of organic acid addition are relative to 20 g of $Fe(NO_3)_3.9H_2O$

2.2 Sediment spiking

Ferrihydrite-organic coprecipitates, representing iron bound organic carbon (OC-Fe_R) were spiked into a OC-free natural sediment sample from the Barents Sea (Water Depth 141 m; sediment core depth, 33.5 cm; station B6, E40; Cruise JR16006) which acted as a 'carrier' for the OC-Fe_R compound and replicated the physical properties of natural fine-grained (silty clay) sediments. The sediment sample was freeze-dried and homogenised by grinding using a pestle and mortar, followed by ashing (650°C, 12 hours) to oxidatively remove all OC. While ashing affects various natural sediment properties (e.g. dehydration/aggregation of

minerals), it is required as a preparatory step in our experiment to remove all natural OC from the sediment. However, the ashed sediment is used simply as a matrix for our OC-Fe_R additions, to better mimic the physical properties of a natural sediment than an artificial mixture of various marine sediment minerals. Inorganic carbon was removed by fumigation with HCl vapour, resulting in a sediment sample dominated by siliciclastic minerals. Spiked samples were prepared by mixing carbon free sediment with ferrihydrite coprecipitates at different ratios (see matrix in **Table 2**) in a centrifuge tube and agitating for 10 minutes at room temperature in light conditions.

Table 2: Concentration matrix for spiked sediments.

%OC-Fe: Sediment	0	10	20	30	40	50
OC-Fe (mg)	0	25	50	75	100	125
Sediment (mg)	250	225	200	175	150	125

Values shown are contextualised for a total experimental sample mass of 250 mg (Lalonde et al., 2012).

2.3 Extraction of iron bound carbon.

Extraction of dithionite reducible Fe_R and associated OC was conducted according to the citrate-dithionite-bicarbonate (CBD) method (Lalonde et al., 2012; Salvadó et al., 2015). Briefly, 0.25 g of spiked sediment was weighed into centrifuge tubes. Following this, 13 ml of 0.11 M sodium bicarbonate ($NaHCO_3$) and 0.27 M trisodium citrate ($Na_3C_6H_5O_7$) solution were added and the mixture pre-heated to 80°C in a water bath. Sodium dithionite (0.25 g) was then dissolved in 2 ml of 0.11 M $NaHCO_3$ and 0.27 M $Na_3C_6H_5O_7$ solution, added, and the mixture was agitated and heated again (80°C, 15 minutes). In parallel, a control extraction was conducted replacing sodium dithionite and trisodium citrate with sodium chloride at an equivalent ionic strength; 13 ml of 1.6 M NaCl and 0.11 M $NaHCO_3$, followed by 0.22 g NaCl dissolved in 2 ml of the NaCl and $NaHCO_3$ solution. All samples were centrifuged (10 minutes) and the supernatant was retained. This was followed by three rinses of the precipitate in artificial seawater with 15 ml of each of these three supernatants retained

and combined with one another. All supernatants were acidified to pH <2 with 12 N HCl to prevent Fe precipitation. Precipitates were oven dried at 60°C for 12 hours and decarbonated by acid fumigation to remove inorganic carbon. Sample mass was recorded prior to elemental analysis to correct for any mass loss.

2.5 Elemental analysis - Iron

Iron concentrations for samples following CBD extraction were determined by atomic absorption spectroscopy (Thermo Fisher iCE3300 AAS). Calibration was performed using matrix matched standards and quality control was confirmed following every 10 samples by repeat sampling of calibration standards to check for drift. Total sedimentary Fe content was determined by digesting ~2 mg of the spiked sediment mixes in 1 ml 12N HCl at room temperature followed by an initial 10-fold dilution with 1% HCl solution. Subsequent dilutions were made, dependent on Fe content, using MilliQ water to produce a subsample within the detectable window (1-10 ppm Fe). Control supernatants were diluted 20-fold to prevent salt blockages and washed supernatants were undiluted except for where the Fe concentration was >10 ppm, whereby these were diluted 10-fold. Extraction of Fe (ΔFe) was calculated as total Fe – CBD extractable Fe, Fe liberated in the NaCl wash stage was subtracted from the CBD extractable total however the NaCl values were negligibly small. Error was determined by propagating the standard error of the mean (SEM) calculated from duplicate results for the total Fe and CBD extractable Fe pools.

2.6 Elemental analysis – Carbon

Initial carbon content of synthetic samples was measured using a LECO-SC144DR C&S analyser. Post extraction carbon was determined by LECO analysis for the majority of sediment samples (OC-Fe concentrations ≤ 50%) or by a Vario PYRO cube (Elementar Analysis) where post extraction sample mass was below the limits required for LECO analysis (OC-Fe concentration >50%). Both instruments were corrected for drift by running a known standard (LECO 502-694 and Elementar sulfanilamide) following every 10-15 samples throughout the

analytical run. All carbon samples were analysed in a dried (oven or freeze-dried) state following the removal of IC as described above. Carbon loss was calculated according to supplementary equation 1, adapted from Peter and Sobek (2018) and Salvadó et al. (2015). Instrument error for C measurement is minimal (≤ 1% RSD) and in all cases was less than the SEM calculated for independent repeat measurements.

2.7 X-Ray diffraction analysis

Ferrihydrite-organic composites were structurally characterised for crystallinity by powder x-ray diffraction (XRD). The pattern was collected over a 2-90° 2θ range in 0.01969° intervals with a step time of 930 ms using a Bruker D8 diffractometer with Cu-Kα radiation source (λ ≈ 0.154 nm). Comparative analysis between the different coprecipitates was achieved by normalising for relative intensity.

2.8 Particle sizing

Sizing of particle aggregates within the range of 0.1-10000 μm was conducted via laser diffraction using a Malvern Mastersizer 2000. Wet ferrihydrite coprecipitates were added dropwise to water in the suspension mixer until within the detection limit of the machine. Detection of the particle scattering pattern was conducted in triplicate by the detector array and interpreted using the Malvern Mastersizer 2000 software (v6.01).

3. Results

3.1 OC content calibration of spiked sediments

Coprecipitation of the three organic acids with ferrihydrite produced coprecipitates with an increasing wt% C content, 1-COOH = 1.15%, 2-COOH = 4.20%, 3-COOH = 8.51%. The molar C/Fe ratio similarly increased (1-COOH = 0.2, 2-COOH = 0.5, 3-COOH = 1). These coprecipitates were then spiked into the treated sediment across a concentration gradient (as detailed in **Table 2**), producing a range of composite samples variable in their C content (**Fig. 2).** The 15 unique sample compositions represent a range of C concentrations from 0.33% (10%, 1-COOH) to 6.94% (50%, 3-COOH). The C content of these

composites varied by both the number of C molecules in the three organic acids and the amount of OC-Fe_R spiked into the sample relative to sediment (see **Table 2**).

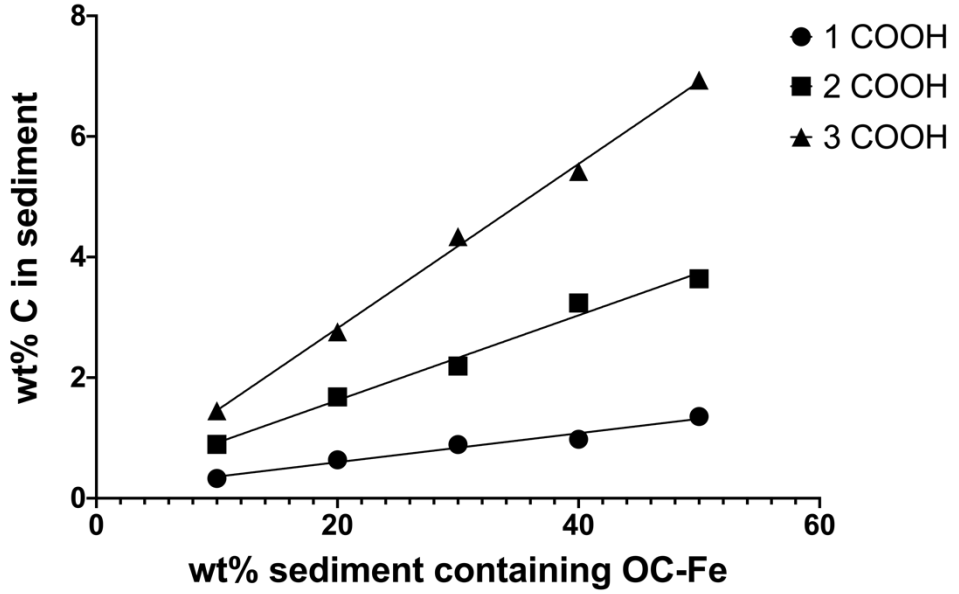

Figure 2 - Calibration of sediment coprecipitate content and sediment wt% C. Coprecipitates show a tight linear regression trend across the series with R-squared values of: 1-COOH = 0.97; 2-COOH = 0.98; 3-COOH = 0.99. 1/2/3 COOH refers to the number of carboxyl groups per molecule in the three different organic acids coprecipitated with ferrihydrite. %C refers to the concentration of carbon in the overall sediment composite by wt%. Instrument error is too small (≤1% RSD) to be visualised.

3.2 Extraction of iron bound organic carbon.

The Fe_R bound OC fraction (%OC-Fe_R) lost from the composite material during the extraction was determined for each of the carboxyl coprecipitate containing samples at concentrations of 20-50% OC-Fe, since C loss for coprecipitates at 10% OC-Fe was too small to be accurately determined (**Fig. 3)**. The wt% C values displayed in black indicate those which have been processed through **Supplementary equation 1**, a minor adaptation to the common equation used to remove OC that is extractable with NaCl and believed to be unbound to Fe_R (Barber et al., 2017; Lalonde et al., 2012; Peter and Sobek, 2018; Salvadó et al., 2015). In blue, the maximal 'true' wt% C extracted are shown, these refer to data which has only been transformed for mass loss, i.e. the control and reduction extractions were not subtracted from one another. For the 1- and 2-COOH samples the value shown in blue represents OC

loss from just the NaCl extraction, as this value was greater than OC loss by dithionite reduction, while for the 3-COOH sample this shows OC loss from reduction as this was higher; all values can be found in **Supplementary table 3**. Consideration of why some samples experienced greater OC loss from treatment with NaCl than by dithionite reduction is explored in **4.1.** Overall, these two sets of values can be grouped separately; the "true" extraction values are similar in nature (shown in the blue box), while the interpreted data (shown in black) become spread after inclusion of both the NaCl control and dithionite reduction values. For the interpreted values ~46% of the total OC-Fe was extracted from the 3-COOH coprecipitate, but 'negative' extractions of ~ -6% and ~ -90% were achieved for the 1- and 2-COOH coprecipitates, respectively. Negative extraction values can be explained as being an artificial feature of subtracting a greater OC loss in the control experiment from a lesser OC loss in the reduction. The mean difference between all three carboxyl coprecipitates was found to be significantly different for all pairwise combinations via a one-way ANOVA and Tukey's test post hoc (99% significance level) **(Supplementary Table S1)**. Precise values for all extractions including duplicate errors are detailed in **Supplementary Table S3.**

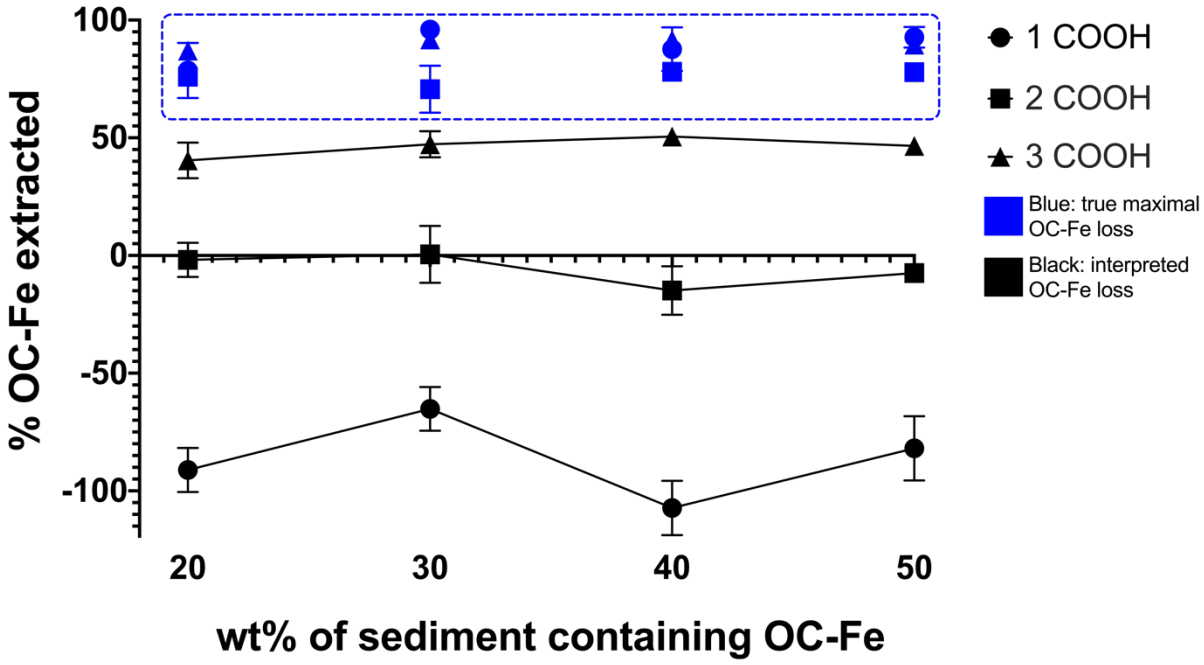

Figure 3- Dithionite extractable fraction of OC from carboxyl coprecipitate spiked sediments. %OC-Fe extracted from artificial sediments spiked with 1,2 or 3 carboxyl organic acids. Error bars show standard error of the mean (SEM) of duplicate values, where error bars are not shown this is because the error is too small to be visualised on this scale. %OC-Fe extracted refers to wt% C removed by reductive dissolution of the reactive iron phase for iron bound carbon. Key descriptors, 1/2/3 COOH, represent the variation in the number of carboxyl groups of the 3 different organic acids coprecipitated with ferrihydrite.

3.3 Iron extraction

Extractable Fe shows an increasing stepwise trend with the number of carboxyl groups per coprecipitated acid molecule for all concentrations of OC-Fe_R relative to sediment **(Fig. 4).** All extractions for easily reducible Fe were incomplete (< 100% of added Fe) with a maximum yield of 61.6% achieved for the 3-COOH coprecipitate at 50% OC-Fe, with a mean range of 50.5-61.6% across all concentrations. In decreasing order, the 2-COOH sediment yield was 40.0-45.7% Fe and 1-COOH sediment yield was 17.9-29.9%. The OC free (0-COOH) sediment composite achieved the lowest rate of Fe recoverability, between 6 and 14%. Fe removed by the NaCl control treatment was subtracted from the Fe removed by CBD, however the contribution of Fe removed by NaCl was minimal (≤ 0.3%). Fe liberated in wash stages for both CBD and NaCl treatment are included in the overall %Fe extracted values. Relative to Fe liberated from the initial chemical treatment, the wash removed a further 6.7-34.0% Fe for CBD and 0.4 to 27.8% for NaCl. All sample means were calculated from the average of independent duplicates. A significant difference was found between the means of all coprecipitate pairwise combinations (>99% significance) by one-way ANOVA analysis and Tukey's test post hoc. A statistical summary is included in **Supplementary Table S2**

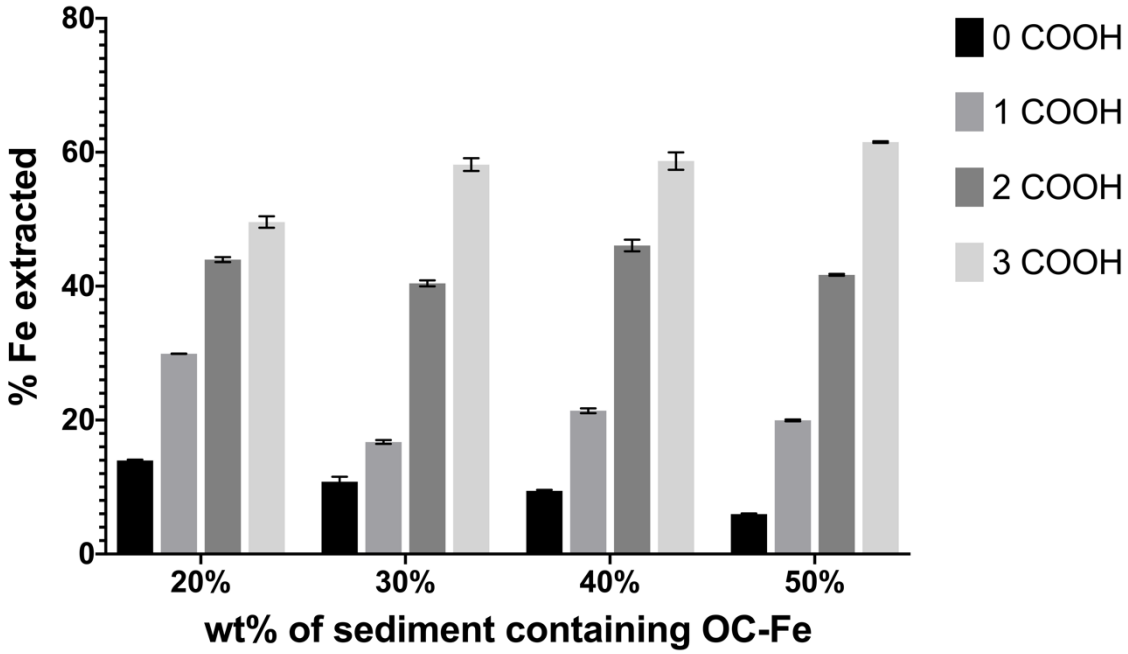

Figure 4- Dithionite Figure 4- CBD extraction efficiency for reactive Fe in sediment samples differing in carboxyl richness. %Fe extracted from each carboxyl spiked sediment (0-3 COOH) is shown, values are control corrected. Error bars represent propagated error calculated from the duplicate values as detailed in 3.1.

3.4 Coprecipitate grain size

Grain size of ferrihydrite composites was determined by laser diffraction analysis in the 0.01 to 10000 μm range. The 3-COOH coprecipitate showed a slight peak shift from 12.04 to 28.66 μm compared to the carboxyl free, pure ferrihydrite phase (0-COOH) **(Fig. 5).** One and two COOH coprecipitates showed no determinable difference in grain size distribution and sat between the 0- and 3-COOH sediments. The 0- and 3-COOH precipitates also had marginally taller, slimmer distributions indicating a narrower range of grain sizes and a greater proportion of the class existed at the mid-point compared to 1- and 2-COOH. These two samples have almost identical normal distribution curves and show no determinable difference in grain size or distribution. Due to the overlapping of all distributions, there is no statistically significant difference in the grain size of coprecipitates.

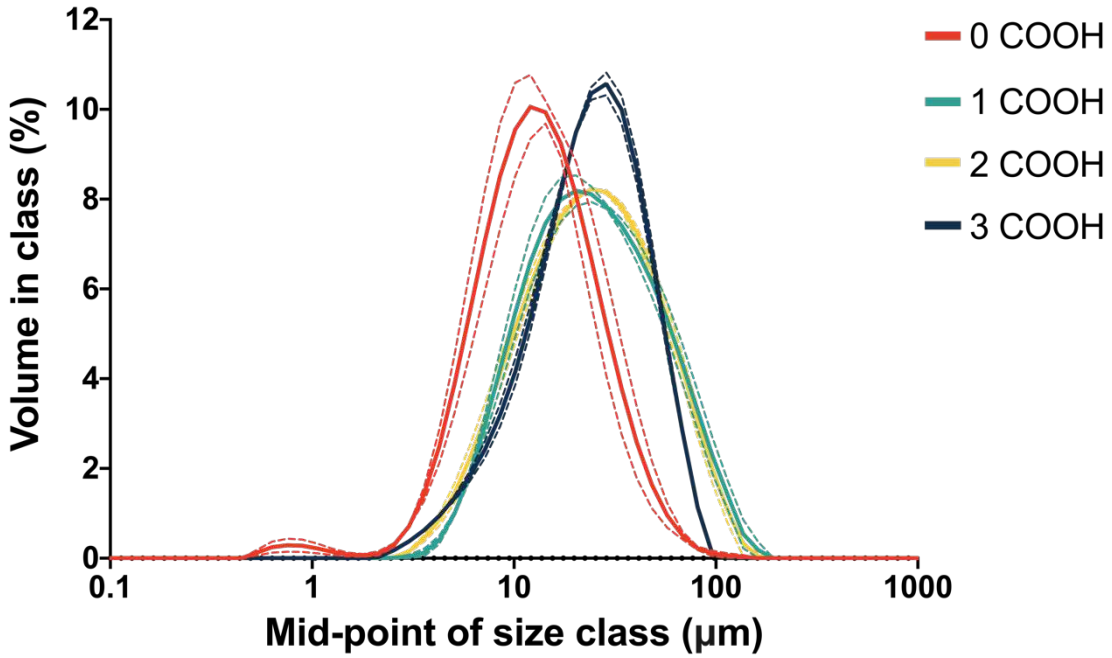

Figure 5- Grain size distribution of carboxyl coprecipitates. Grain size distribution is shown as percent by volume in class. Values shown along the solid lines are the mean of triplicate measurements, dashed lines represent the SEM. A small number of data points in the range 0.01-0.1 µm and 1000-10000 µm are excluded from this graph to improve resolution, all these values were ~0.

3.5 X-ray diffraction analysis (XRD)

All samples show a characteristic two peak signature **(Supplementary Fig. S1)**, indicating successful synthesis, and carboxyl free ferrihydrite resembles a characteristic two-line sample. As the number of carboxyl groups per coprecipitated acid molecule increases, a decrease in relative intensity and softening of the two peaks can be seen.

4. Discussion

Organic carbon bound to Fe_R represents an important mechanism by which OC is preserved in marine sediments with ~22% of total sediment OC bound to Fe_R (Lalonde et al., 2012). This “rusty sink” is important for regulating atmospheric O_2 and CO_2 (Torn et al., 1997) and understanding the fate of OM is crucial in accurately predicting the future of carbon cycling under global climate change (Adhikari and Yang, 2015). The CBD method, previously used to quantify OC-Fe_R in terrestrial environments, has been applied to marine sediments providing the first quantification of OC preserved in association with Fe_R on a global scale (Lalonde et al.,

2012). Here we applied the same CBD method to synthetic samples, in an experimental investigation of OC-Fe_R, to investigate the performance of the CBD method for OC and Fe extractability as a function of the molecular characteristics of the associated OM. Previous studies have typically produced organomineral coprecipitates using natural sources of OM, e.g., forest floor extract (Chen et al., 2014; Eusterhues et al., 2014a; Eusterhues et al., 2014b; Eusterhues et al., 2011). Whilst using naturally sourced OM more closely replicates OC-Fe_R coprecipitates formed in environmental settings, the speciation and structure of natural OM are largely unknown and therefore the effect of OM molecular composition on the efficiency of the CBD method cannot be easily evaluated. By using short chain organic molecules, differing only in the number of carboxyl groups per acid molecule, we explore how the CBD method is influenced by the carboxylic character of the OM. We demonstrate important inefficiencies in the CBD method through calibration against synthetic standards which has the potential to transform our interpretation of CBD extractions performed on natural sediments and thus our understanding of marine sediment carbon preservation on a global scale **(4.1, 4.2).** We also comment on how the carboxyl character of the OM might have a significant influence on OM preservation **(4.3).**

4.1 Current extraction methods may underestimate the extent of OC-Fe_R interactions in soils and sediments

Preservation of OM by Fe_R is thought to result from protection of OC from microbial degradation, mediated through chemical bonding between OC and Fe_R (Kaiser and Guggenberger, 2000). Protection is believed to require high energy bonding between OC and Fe_R to maintain a preservative effect (Henrichs, 1995). Weaker interactions (e.g., Van der Waals forces) may exist but are assumed to be of insufficient strength to facilitate OM preservation (Burdige, 2007). Treatment with CBD has been described to dissolve “all solid reactive iron phases and the organic carbon associated with these phases” in natural sediments (Lalonde et al., 2012). Therefore, we would expect full liberation of Fe and C given that the C content of our synthetic sample was equal to the amount of OC

associated with ferrihydrite, a solid reactive Fe phase. Across all concentrations and C structures we observe incomplete recovery of Fe_R, not exceeding 50.51 ± 1.32% of the added Fe content (3-COOH, 40% OC-Fe_R addition) **(Fig. 2)**. As the amount of OC extracted is less than total amount of OC added to the sediment samples this indicates either the CBD method or the interpretation of CBD results contain a source of error. However, the OC-Fe_R values obtained, in particular for the 3-COOH containing sediment, are comparable to observations from many environmental samples.

Where CBD has been applied to marine sediments the %OC-Fe_R (= fraction of total OC bound to Fe_R) ranges between 0-42% on continental shelves (e.g. Lalonde et al., 2012; Ma et al., 2018; Salvadó et al., 2015) with typical averages for sediments under oxic bottom waters of 21.7 ± 7.8% (Lalonde et al., 2012). While the calculation for our 3-COOH coprecipitate exceeds these ranges for %OC-Fe_R in marine sediments, it is agreeable with terrestrial environments. For example, Zhao et al. (2016) determined an %OC-Fe_R pool of 37.8 ± 20% for forest soils. The appearance of a less than complete OC extraction might be explained by the large loss of OC-Fe_R from NaCl treatment, designed to remove OC not bound to Fe_R. Lalonde et al. (2012) note 7.2 ± 5.4% of OC is released from treatment of natural sediments with NaCl, while we recorded 43.81 ± 3.06% for our 3-COOH coprecipitate. The subtraction of this OC pool, thought to be unbound to Fe_R, reduces the value for %OC-Fe_R from 90.00 ± 2.50 % removed by CBD treatment to 46.19 ± 7.57 %. Therefore, we suggest that OC removed by CBD gives a more accurate assessment of OC-Fe_R, and that the subtraction of the NaCl 'control' pool in previous studies may have led to a severe underestimation of the actual size of the %OC-Fe_R pool.

The effect of NaCl removal of OC is amplified for the 1- and 2-COOH sediment composites compared to the 3-COOH composite. Here, the substantial extraction of OC by NaCl results in final %OC-Fe_R calculations of ~-90% and ~-6% respectively (**Fig. 2),** which is physically implausible.

This demonstrates that the NaCl control treatment is capable of removing OC from a Fe_R mineral interface. While the effect of NaCl on the OC-Fe_R association has not been previously investigated and is largely based on assumptions, research in soils has indicated that NaCl has the ability to interfere with Fe_R minerals, with Pereira et al. (2019) showing that 8-10% of Na^+ and Cl^- ions in a NaCl solution can adsorb to ferrihydrite. Subsequently the presence of NaCl can affect the adsorption kinetics of organic compounds to Fe_R with a positive relationship observed between increasing NaCl concentration and adsorption of glyphosate (an organic herbicide) to ferrihydrite (Pereira et al., 2019), while (Orcelli et al., 2018) show an inverse trend for glyphosate adsorption to goethite.

In our study we are able to show NaCl is capable of removing OC-Fe_R because by synthesising coprecipitates, we have ensured that all OC in the sample is associated with Fe_R: i) ferrihydrite is the only reactive interface OC is exposed to; ii) residual OC not associated with ferrihydrite is already removed by multiple rinses following precipitation, at which point C/Fe ratio determination is recommended (Eusterhues et al., 2011; Han et al., 2019). Presumably C/Fe determination would not be recommended following rinses if it was plausible that non-Fe associated OC remained in the coprecipitate, as this would skew these ratios by including excess OC.

In addition to a high OC loss in the control, we may also be observing an artificially low OC loss in the CBD treatment stage. This can explain negative mean values for C% loss of -12.53% and -19.61% following CBD extraction at 20 and 40% (1-COOH), respectively. Under reducing conditions, the Fe_R phase is dissolved by sodium dithionite and the coprecipitate experiences Fe loss, as shown in **Fig. 4**. However, this Fe loss is incomplete and much of the phase (~77%) remains within the sediment. Liberation of OC from the surface of ferrihydrite during reductive dissolution will increase the number of available surface binding sites and therefore could allow for either re-adsorption of liberated OC or sorption of C containing reagents involved in the reduction stage (sodium

519 bicarbonate, trisodium citrate). While sorption of bicarbonate to Fe
520 (hydr)oxides at neutral pH is a thermodynamically favourable process via
521 monodentate inner-sphere complexation (Acelas et al., 2017),
522 bicarbonate contamination is not expected to be significant due to acid
523 fumigation of samples to remove carbonates. Lalonde et al. (2012) also
524 determined residual bicarbonate to be insignificant, contributing ≤ 0.08%
525 of dry sediment weight. Sorption of OC or citrate onto reduced Fe_R phases
526 could elevate the sediment carbon concentration determined and
527 therefore appear to artificially decrease %C loss in the reduction stage,
528 below what is observed in the non-dissolved control.
529
530 The CBD method assumes that treatment of sediment with NaCl removes
531 OC not associated with Fe_R. However, our results suggest that this NaCl
532 leached pool of OC is bound to Fe_R phases but less strongly than the CBD
533 extractable pool, with the susceptibility of an individual OC compound
534 towards removal with NaCl being linked to its carboxyl content. The extent
535 to which comparatively weak OC-Fe_R associations, removed from Fe_R by
536 NaCl, confer protection from microbial degradation upon OC is unknown,
537 however, a large co-localisation of OC with mineral phases (including Fe)
538 has been observed at depths far beyond quantification of OC-Fe_R (23.9
539 metres below seafloor) (Estes et al., 2019). This potentially suggests the
540 extent of OC association with Fe_R is larger than determined by CBD
541 extraction. We suggest that the OC pool extractable by NaCl is of
542 importance when calculating the overall OC-Fe_R budget. The scale of this
543 importance is demonstrated by the additional 7.2 ± 5.4% OC removed
544 with NaCl in treatment of surface marine sediment, previously exposed to
545 seawater (Lalonde et al., 2012). When accounting for the mass of C lost
546 in the extraction (as in this study and in Salvadó et al. (2015)) the removal
547 of OC by NaCl is even greater with 16.4%±7.1% of OC-Fe_R being
548 discounted from an initial CBD extraction of 27.4%±5.4% (Salvadó et al.,
549 2015). Therefore, the subtraction of OC removed by NaCl from the overall
550 OC-Fe pool has a large influence on the resulting value for OC-Fe_R
551 calculation. It is a question as to why exposure to NaCl should remove
552 such a large fraction of OC from marine sediments which have existed in

environments surrounded by seawater for many years. However, the NaCl wash employed in the CBD method is of a much greater molar strength than seawater (1.85 M vs 0.49 M). Our results show that NaCl treatment does have the ability to remove Fe_R bound OC and therefore subtraction of this value from CBD extractions has the potential to underestimate the global OC-Fe_R budget. Given the ability of NaCl to remove loosely bound OC, caution should be taken in interpreting OC extracted in this way before removal from the dithionite extractable pool.

A recalculation on the presumption that all NaCl removable OC extracted by Lalonde et al. (2012) represents weakly bound OC-Fe_R suggests that the role of Fe_R in preserving OC could be underestimated by up to ~33%. However, while in a synthetic experiment it appears that NaCl removable OC is bound to Fe_R phases, this may not be fully translated to natural sediments due to the loss of OC from other sources, such as those bound to manganese oxides and other mineral surfaces (Allard et al., 2017; Bernard, 1997; Tipping and Heaton, 1983) or DOC dissolved in the pore waters (Fox et al., 2018; Rossel et al., 2016). A change in the extent to which OC-Fe_R contributes to OM preservation has ramifications for both the global OC-Fe_R budget and for biogeochemical models aiming to include OM preservation mechanisms to reduce uncertainties related to the fate of OM (Schmidt et al., 2011; Zhao et al., 2016) . The bias towards removal of organic compounds with a lower number of carboxyl groups by NaCl suggests that these moieties are the most likely organic compounds to be excluded from OC-Fe_R quantifications by the CBD method. However, the underlying mechanisms controlling OC-Fe_R bonding and the strength of these OC-Fe_R bonds requires further investigation.

4.2 Current extraction methods may incompletely extract reactive iron phases in sediments.

Quantifying the efficiency of Fe_R extraction techniques has largely been neglected within the literature due to the nature of chemical methods being operationally defined, making it difficult to calibrate these against alternative methods of measuring Fe_R phases such as Mössbauer

spectroscopy (Hepburn et al., 2020). In marine sediments, total Fe is comprised of phases of differing stability, requiring extraction techniques of increasing strength to remove them (Poulton and Canfield, 2005). Here we isolated ferrihydrite, which is considered easily reducible by sodium dithionite as part of the Fe_R pool (Lalonde et al., 2012). However, our measure of Fe extractability shows a maximum extraction of only ~60 wt% Fe when coprecipitated with a 3-COOH acid; comparable with the incomplete (~31-50%) sodium dithionite reduction of hematite-humic acid complexes observed by Adhikari and Yang (2015). We find that Fe extractability appears to be even less efficient, for 1- and 2-COOH coprecipitates (**Fig. 4).**

While reduction by Na dithionite is a well-established method, the adoption of CBD treatment at circumneutral pH, to avoid hydrolysis of OC, remains unique to the OC extraction application. Thompson et al. (2019) found that a CBD extraction at pH 7.6 fails to extract a large proportion of crystalline Fe oxide minerals in both modern and ancient sedimentary rocks. We make a similar observation for OC-free ferrihydrite phases, where only 9.91 ± 0.95% Fe is recovered post extraction. While it is apparent that CBD treatment cannot fully extract easily reducible Fe (hydr)oxide phases, and therefore the entire associated OC pool, there is no obvious improvement that can be made to the current protocol due to the constraints of maintaining a neutral pH.

The apparent trend between the number of carboxyl groups per coprecipitated acid molecule and Fe extracted **(Fig. 2)** may be explained by considering how the association of OC with iron (hydr)oxides effects the structural order of the resulting mineral phases. Previous work shows that with increasing OC content, the mineral is more poorly ordered (Cismasu et al., 2011; Mikutta, 2011; Mikutta et al., 2008). Thus, because we see increased OC uptake with the number of carboxyl groups per acid molecule, it is expected that our ferrihydrite becomes more poorly ordered and thus less chemically stable compared to OC-free ferrihydrite. Our XRD analysis supports this theory as a weakening of peaks identifying 2-

line ferrihydrite is observed when OC content in the coprecipitates is increased **(Supplementary Fig. S1)**. Decreasing crystallinity was similarly observed for samples where total OC (polygalacturonic acid) content was increased (C/Fe 0-2.5) which inhibits transformation of ferrihydrite to more stable phases (ThomasArrigo et al., 2018). In addition, upon extraction the presence of organic matter in OM-Fe_R complexes has previously been attributed to the reductive release of Fe through electron shuttling effects, due to the ability of organic compounds to act as electron carriers between redox reactions (Adhikari and Yang, 2015).

4.3 Carboxyl content of Fe associated OC effects OC extraction

As the carboxyl content of our coprecipitates increases, the ability of dithionite to remove OC increases, while the ability of NaCl to remove OC diminishes. For the sample spiked with 50% OC-Fe, the 1-COOH sample was extractable for 92.74 ± 4.39% of its OC-Fe content by treatment with NaCl while dithionite removed only 10.85 ± 9.32% **(Supplementary Table S3.)** The balance between OC liberated by dithionite vs NaCl subsequently shifts in favour of dithionite with increasing carboxyl content, for the 2-COOH sample the values are roughly equal (dithionite = 70.42 ± 1.23%, NaCl = 77.89 ± 2.12%). Finally, for the 3-COOH sample dithionite is twice as effective than NaCl, removing 89.60 ± 0.49% of OC compared to 43.04 ± 0.49%, the trend described for the 50% OC-Fe sample was similarly observed across all coprecipitate concentrations **(Fig. 3).**

It is assumed that NaCl is only likely to remove weakly bound OC, since OC-Fe bonds are known to be very strong (Barber et al., 2017; Henrichs, 1995) and NaCl was previously attributed to only removing OC not associated with Fe_R (Lalonde et al., 2012). Further, the extraction of less OC from sediments upon treatment with NaCl compared to dithionite (e.g. Lalonde et al., 2012; Salvadó et al., 2015) demonstrates that the NaCl treatment must be less aggressive than dithionite, which is to be expected since NaCl has no reducing power. Therefore, the greater loss of OC by NaCl treatment compared to dithionite for the 1- and 2-COOH containing samples suggests a greater proportion of this OC is weakly bound

655 compared to the 3-COOH sample. In turn this suggests that polycarboxylic
656 acids and more carboxyl rich compounds are more strongly bound to Fe_R,
657 possibly via the formation of multiple strong carboxyl ligand exchange
658 bonds, and hence that carboxyl rich OM might be preferentially preserved
659 in soils and sediments (Kaiser and Guggenberger, 2007).
660
661 For our coprecipitation experiments, the OC source was isolated to
662 carboxyl groups as far as possible, with unavoidable inclusion of one
663 additional short chain C molecule in the 1- and 2-COOH acids (4 non-
664 COOH C's) compared to the 3-COOH acid (3 non-COOH C's). As COOH
665 and OH groups are thought to be important for OM-Fe binding (Karlsson
666 and Persson, 2010; Karlsson and Persson, 2012; Mikutta, 2011; Yang et
667 al., 2012) individual moieties of carboxylic acid were used to reproduce
668 natural OM binding to Fe_R, but in a controlled system where the potential
669 for different sorption mechanisms due to different OM functional groups
670 was reduced. If polycarboxylic acids and more carboxyl rich OM
671 compounds are more strongly bound to Fe_R then environmental conditions
672 favouring high concentrations of Fe, such as continental margins and
673 hydrothermal vents (Tagliabue et al., 2017), as well as carboxyl rich OM
674 inputs (e.g., regions of high primary productivity and shallow waters) are
675 likely to be more efficient at preserving OC.
676
677 The translation of this implication into an environmental context requires
678 an understanding of the moieties present in marine DOM. Much of the
679 work aimed at probing the OC-Fe_R interaction has involved
680 coprecipitations of Fh with terrestrial DOM (e.g., Eusterhues et al., 2014a;
681 Eusterhues et al., 2014b; Eusterhues et al., 2011). Typical coprecipitation
682 experiments for Fe_R bound OC use DOM from forest floor extracts or
683 standards (e.g., Suwannee River). Molecular level work using scanning
684 transmission X-ray microscopy coupled with near-edge X-ray absorption
685 fine structure (STXM NEXAFS) spectroscopy suggests the importance of
686 OM carboxyl content for OC binding to Fe_R by using forest floor extract
687 enriched for carboxyl content (Chen et al. (2014). Coprecipitation with
688 terrestrial organic matter may not be representative of marine DOM

however, as marine DOM might be enriched in carboxyl content, for example, a significant fraction of refractory marine DOM is composed of carboxyl-rich alicyclic molecules 'CRAM' (Hertkorn et al., 2006). Additionally, marine (algae) OM further differs from terrestrial sources by exhibiting a lower C/N ratio (4-10) than terrestrial OM (>20) (Meyers, 1994). Higher plants, the largest contributor to terrestrial OM, contain less than 20% protein, hence have lower nitrogen contents and higher C/N ratios than protein rich (~80%) marine bacteria and benthic animals (Müller, 1977). OM preserved in ancient sediments (since 11.6 Ma) shows increased C/N ratios (>10) relative to marine surface (algal) OM (Twichell et al., 2002). This change is attributed to partial OM degradation during sinking and potentially post deposition. Verardo and McIntyre (1994), however, suggest that alteration of C/N ratios from shallow to deep burial in sediments occurs due to favourable decomposition of N-rich (C/N low) OM by microbial communities. This would imply that N-rich (C/N low) marine OM undergoes more extensive structural alteration during decomposition than C/N high terrestrial OM. Future work should focus on coprecipitation of carboxyl rich OM and marine OM with Fe_R to further elucidate the controls on OC-Fe_R associations.

5.0 Conclusion

Determining of the amount of OM associated with Fe_R in sediments is an important parameter in understanding the fate of OM in the marine environment and the biogeochemical controls on the global C cycle more widely. Currently, only the CBD method exists for quantifying the extent of this interaction, however, by estimating OC-Fe_R using a chemical extraction, this means any resulting value is operationally defined by its susceptibility to chemical treatment and not by its persistence or association with Fe_R. Despite this uncertainty, little work had been performed to understand the limitations of the CBD method and therefore results are currently considered to be representing all of the Fe_R and associated OC in a sediment sample, with some studies using this value to estimate regional or global OC-Fe_R budgets. Here, we performed CBD extractions on synthetic ferrihydrite-organic acid coprecipitates varying in

their carboxyl context to understand how samples which should be recoverable for their total Fe and C contents performed under the CBD method. In contrast with assertions that CBD treatment was able to fully reduce all solid Fe_R phases and associated OC, we found that CBD is unable to fully reduce ferrihydrite. Further, we show Fe reduction to be variable based on the chemical composition of OM, specifically carboxyl group content. As an increasing number of carboxyl groups become associated with a ferrihydrite-organic coprecipitate this exerts a strong control on the crystallinity and therefore reactivity of Fe, with a significant increase in the amount of Fe reduced for carboxyl rich coprecipitates. Additionally, we found that the NaCl wash stage has the ability to remove a large amount of Fe bound OM and that further consideration should be given in interpreting OC loss from the NaCl stage before subtracting this, often large value, from the dithionite extractable pool. These conclusions have significant implications for the quantification of OC-Fe_R as NaCl extractable OC was originally thought to only extract non-Fe bound OC and therefore this sum is subtracted from the dithionite extractable pool of OC-$Fe_{R.}$ Our results therefore indicate that a combination of incomplete Fe_R reduction by CBD and removal of Fe_R bound OC by NaCl have likely contributed towards an underestimation of the extent to which OC-Fe_R interactions persist in marine sediments.

Acknowledgements

This work was supported by funds from the ChAOS project (NE/P006493/1), part of the Changing Arctic Ocean programme, jointly funded by the UKRI Natural Environment Research Council (NERC) and the German Federal Ministry of Education and Research (BMBF). Additionally, this research project has received funding from the European Research Council (ERC) under the European Union's Horizon 2020 research and innovation programme (Grant agreement No. 725613 MinOrg). We thank two anonymous reviewers for their constructive feedback which improved the final manuscript.

References

Acelas, N.Y., Hadad, C., Restrepo, A., Ibarguen, C., Florez, E., 2017. Adsorption of Nitrate and Bicarbonate on Fe-(Hydr)oxide. Inorg Chem, 56(9): 5455-5464, https://doi.org/10.1021/acs.inorgchem.7b00513.

Adhikari, D., Yang, Y., 2015. Selective stabilization of aliphatic organic carbon by iron oxide. Sci Rep, 5(1): 11214, https://doi.org/10.1038/srep11214.

Allard, S., Gutierrez, L., Fontaine, C., Croue, J.P., Gallard, H., 2017. Organic matter interactions with natural manganese oxide and synthetic birnessite. Sci Total Environ, 583: 487-495, https://doi.org/10.1016/j.scitotenv.2017.01.120.

Arndt, S. et al., 2013. Quantifying the degradation of organic matter in marine sediments: A review and synthesis. Earth-Science Reviews, 123: 53-86, https://doi.org/10.1016/j.earscirev.2013.02.008.

Barber, A. et al., 2017. Preservation of organic matter in marine sediments by inner-sphere interactions with reactive iron. Sci Rep, 7(1): 366, https://doi.org/10.1038/s41598-017-00494-0.

Bernard, S., 1997. Removal of organic compounds by adsorption on pyrolusite (β-MnO2). Water Research, 31(5): 1216-1222, https://doi.org/10.1016/s0043-1354(96)00149-2.

Berner, R.A., 1989. Biogeochemical cycles of carbon and sulfur and their effect on atmospheric oxygen over phanerozoic time. Palaeogeography, Palaeoclimatology, Palaeoecology, 75(1): 97-122, https://doi.org/https://doi.org/10.1016/0031-0182(89)90186-7.

Burdige, D.J., 2007. Preservation of organic matter in marine sediments: controls, mechanisms, and an imbalance in sediment organic carbon budgets? Chem Rev, 107(2): 467-85, https://doi.org/10.1021/cr050347q.

Canfield, D.E., 1994. Factors influencing organic carbon preservation in marine sediments. Chem Geol, 114(3-4): 315-29, https://doi.org/10.1016/0009-2541(94)90061-2.

Chen, C., Dynes, J.J., Wang, J., Sparks, D.L., 2014. Properties of Fe-organic matter associations via coprecipitation versus adsorption. Environ Sci Technol, 48(23): 13751-9, https://doi.org/10.1021/es503669u.

Cismasu, A.C., Michel, F.M., Tcaciuc, A.P., Tyliszczak, T., Brown, J.G.E., 2011. Composition and structural aspects of naturally occurring ferrihydrite. Comptes Rendus Geoscience, 343(2-3): 210-218, https://doi.org/10.1016/j.crte.2010.11.001.

Estes, E.R. et al., 2019. Persistent organic matter in oxic subseafloor sediment. Nature Geoscience, 12(2): 126-131, https://doi.org/10.1038/s41561-018-0291-5.

Eusterhues, K. et al., 2014a. Reduction of ferrihydrite with adsorbed and coprecipitated organic matter: microbial reduction by Geobacter bremensis vs. abiotic reduction by Na-dithionite. Biogeosciences, 11(18): 4953-4966, https://doi.org/10.5194/bg-11-4953-2014.

Eusterhues, K., Neidhardt, J., Hädrich, A., Küsel, K., Totsche, K.U., 2014b. Biodegradation of ferrihydrite-associated organic matter. Biogeochemistry, 119(1-3): 45-50, https://doi.org/10.1007/s10533-013-9943-0.

Eusterhues, K. et al., 2011. Fractionation of organic matter due to reaction with ferrihydrite: coprecipitation versus adsorption. Environ Sci Technol, 45(2): 527-33, https://doi.org/10.1021/es1023898.

Fox, C.A., Abdulla, H.A., Burdige, D.J., Lewicki, J.P., Komada, T., 2018. Composition of Dissolved Organic Matter in Pore Waters of Anoxic Marine Sediments Analyzed by 1H Nuclear Magnetic Resonance Spectroscopy. Frontiers in Marine Science, 5(172), https://doi.org/10.3389/fmars.2018.00172.

Gu, B., Schmitt, J., Chen, Z., Liang, L., McCarthy, J.F., 1994. Adsorption and desorption of natural organic matter on iron oxide: mechanisms and models. Environ Sci Technol, 28(1): 38-46, https://doi.org/10.1021/es00050a007.

Gu, B., Schmitt, J., Chen, Z., Liang, L., McCarthy, J.F., 1995. Adsorption and desorption of different organic matter fractions on iron oxide. Geochimica et Cosmochimica Acta, 59(2): 219-229, https://doi.org/10.1016/0016-7037(94)00282-q.

Han, L. et al., 2019. Mobilization of ferrihydrite-associated organic carbon during Fe reduction: Adsorption versus coprecipitation. Chemical Geology, 503: 61-68, https://doi.org/10.1016/j.chemgeo.2018.10.028.

Hedges, J.I., Keil, R.G., 1995. Sedimentary organic matter preservation: an assessment and speculative synthesis. Marine Chemistry, 49(2-3): 81-115, https://doi.org/10.1016/0304-4203(95)00008-f.

Hemingway, J.D., Rothman, D.H., Rosengard, S.Z., Galy, V.V., 2017. Technical note: An inverse method to relate organic carbon reactivity to isotope composition from serial oxidation. Biogeosciences, 14(22): 5099-5114, https://doi.org/10.5194/bg-14-5099-2017.

Henneberry, Y.K., Kraus, T.E.C., Nico, P.S., Horwath, W.R., 2012. Structural stability of coprecipitated natural organic matter and ferric iron under reducing conditions. Organic Geochemistry, 48: 81-89, https://doi.org/10.1016/j.orggeochem.2012.04.005.

Henrichs, S.M., 1995. Sedimentary organic matter preservation: an assessment and speculative synthesis—a comment. Marine Chemistry, 49(2): 127-136, https://doi.org/https://doi.org/10.1016/0304-4203(95)00012-G.

Hepburn, L.E., Butler, I.B., Boyce, A., Schröder, C., 2020. The use of operationally-defined sequential Fe extraction methods for mineralogical applications: A cautionary tale from Mössbauer spectroscopy. Chemical Geology, 543, https://doi.org/10.1016/j.chemgeo.2020.119584.

Hertkorn, N. et al., 2006. Characterization of a major refractory component of marine dissolved organic matter. Geochimica et Cosmochimica Acta, 70(12): 2990-3010, https://doi.org/10.1016/j.gca.2006.03.021.

Jones, D.L., Edwards, A.C., 1998. Influence of sorption on the biological utilization of two simple carbon substrates. Soil Biology and Biochemistry, 30(14): 1895-1902, https://doi.org/10.1016/s0038-0717(98)00060-1.

Kaiser, K., Guggenberger, G., 2000. The role of DOM sorption to mineral surfaces in the preservation of organic matter in soils. Organic Geochemistry, 31(7-8): 711-725, https://doi.org/10.1016/s0146-6380(00)00046-2.

Kaiser, K., Guggenberger, G., 2007. Sorptive stabilization of organic matter by microporous goethite: sorption into small pores vs. surface complexation.

European Journal of Soil Science, 58(1): 45-59, https://doi.org/10.1111/j.1365-2389.2006.00799.x.
Karlsson, T., Persson, P., 2010. Coordination chemistry and hydrolysis of Fe(III) in a peat humic acid studied by X-ray absorption spectroscopy. Geochimica et Cosmochimica Acta, 74(1): 30-40, https://doi.org/10.1016/j.gca.2009.09.023.
Karlsson, T., Persson, P., 2012. Complexes with aquatic organic matter suppress hydrolysis and precipitation of Fe(III). Chemical Geology, 322-323: 19-27, https://doi.org/10.1016/j.chemgeo.2012.06.003.
Lalonde, K., Mucci, A., Ouellet, A., Gelinas, Y., 2012. Preservation of organic matter in sediments promoted by iron. Nature, 483(7388): 198-200, https://doi.org/10.1038/nature10855.
Ma, W.-W., Zhu, M.-X., Yang, G.-P., Li, T., 2018. Iron geochemistry and organic carbon preservation by iron (oxyhydr)oxides in surface sediments of the East China Sea and the south Yellow Sea. Journal of Marine Systems, 178: 62-74, https://doi.org/10.1016/j.jmarsys.2017.10.009.
Meyers, P.A., 1994. Preservation of elemental and isotopic source identification of sedimentary organic matter. Chemical Geology, 114(3-4): 289-302, https://doi.org/10.1016/0009-2541(94)90059-0.
Michel, F.M. et al., 2007. The Structure of Ferrihydrite, a Nanocrystalline Material. Science, 316(5832): 1726-1729, https://doi.org/10.1126/science.1142525.
Mikutta, C., 2011. X-ray absorption spectroscopy study on the effect of hydroxybenzoic acids on the formation and structure of ferrihydrite. Geochimica et Cosmochimica Acta, 75(18): 5122-5139, https://doi.org/10.1016/j.gca.2011.06.002.
Mikutta, C. et al., 2008. Synthetic coprecipitates of exopolysaccharides and ferrihydrite. Part I: Characterization. Geochimica et Cosmochimica Acta, 72(4): 1111-1127, https://doi.org/10.1016/j.gca.2007.11.035.
Mu, C.C. et al., 2016. Soil organic carbon stabilization by iron in permafrost regions of the Qinghai-Tibet Plateau. Geophysical Research Letters, 43(19): 10,286-10,294, https://doi.org/10.1002/2016gl070071.
Müller, P.J., 1977. CN ratios in Pacific deep-sea sediments: Effect of inorganic ammonium and organic nitrogen compounds sorbed by clays. Geochimica Et Cosmochimica Acta, 41(6): 765-776, https://doi.org/http://dx.doi.org/10.1016/0016-7037(77)90047-3.
Orcelli, T. et al., 2018. Study of Interaction Between Glyphosate and Goethite Using Several Methodologies: an Environmental Perspective. Water, Air, & Soil Pollution, 229(5): 150, https://doi.org/10.1007/s11270-018-3806-1.
Pereira, R.C. et al., 2019. The effect of pH and ionic strength on the adsorption of glyphosate onto ferrihydrite. Geochemical Transactions, 20(1): 3, https://doi.org/10.1186/s12932-019-0063-1.
Peter, S., Sobek, S., 2018. High variability in iron-bound organic carbon among five boreal lake sediments. Biogeochemistry, 139(1): 19-29, https://doi.org/10.1007/s10533-018-0456-8.
Poulton, S.W., Canfield, D.E., 2005. Development of a sequential extraction procedure for iron: implications for iron partitioning in continentally derived particulates. Chemical Geology, 214(3-4): 209-221, https://doi.org/10.1016/j.chemgeo.2004.09.003.

Raiswell, R., Canfield, D.E., Berner, R.A., 1994. A comparison of iron extraction methods for the determination of degree of pyritisation and the recognition of iron-limited pyrite formation. Chem Geol, 111(1-4): 101-10, https://doi.org/10.1016/0009-2541(94)90084-1.

Rossel, P.E., Bienhold, C., Boetius, A., Dittmar, T., 2016. Dissolved organic matter in pore water of Arctic Ocean sediments: Environmental influence on molecular composition. Organic Geochemistry, 97: 41-52, https://doi.org/https://doi.org/10.1016/j.orggeochem.2016.04.003.

Salvadó, J.A. et al., 2015. Organic carbon remobilized from thawing permafrost is resequestered by reactive iron on the Eurasian Arctic Shelf. Geophysical Research Letters, 42(19): 8122-8130, https://doi.org/10.1002/2015gl066058.

Schmidt, M.W. et al., 2011. Persistence of soil organic matter as an ecosystem property. Nature, 478(7367): 49-56, https://doi.org/10.1038/nature10386.

Tagliabue, A. et al., 2017. The integral role of iron in ocean biogeochemistry. Nature, 543(7643): 51-59, https://doi.org/10.1038/nature21058.

ThomasArrigo, L.K., Byrne, J.M., Kappler, A., Kretzschmar, R., 2018. Impact of Organic Matter on Iron(II)-Catalyzed Mineral Transformations in Ferrihydrite-Organic Matter Coprecipitates. Environ Sci Technol, 52(21): 12316-12326, https://doi.org/10.1021/acs.est.8b03206.

Thompson, J. et al., 2019. Development of a modified SEDEX phosphorus speciation method for ancient rocks and modern iron-rich sediments. Chemical Geology, 524: 383-393, https://doi.org/10.1016/j.chemgeo.2019.07.003.

Tipping, E., Heaton, M.J., 1983. The adsorption of aquatic humic substances by two oxides of manganese. Geochimica et Cosmochimica Acta, 47(8): 1393-1397, https://doi.org/10.1016/0016-7037(83)90297-1.

Torn, M.S., Trumbore, S.E., Chadwick, O.A., Vitousek, P.M., Hendricks, D.M., 1997. Mineral control of soil organic carbon storage and turnover. Nature, 389(6647): 170-173, https://doi.org/10.1038/38260.

Twichell, S.C., Meyers, P.A., Diester-Haass, L., 2002. Significance of high C/N ratios in organic-carbon-rich Neogene sediments under the Benguela Current upwelling system. Organic Geochemistry, 33(7): 715-722, https://doi.org/10.1016/s0146-6380(02)00042-6.

Verardo, D.J., McIntyre, A., 1994. Production and destruction: Control of biogenous sedimentation in the tropical Atlantic 0–300,000 years BP. Paleoceanography, 9(1): 63-86,

Wagai, R., Mayer, L.M., 2007. Sorptive stabilization of organic matter in soils by hydrous iron oxides. Geochimica et Cosmochimica Acta, 71(1): 25-35, https://doi.org/10.1016/j.gca.2006.08.047.

Yang, Y., Takizawa, S., Sakai, H., Murakami, M., Watanabe, N., 2012. Removal of organic matter and phosphate using ferrihydrite for reduction of microbial regrowth potential. Water Sci Technol, 66(6): 1348-53, https://doi.org/10.2166/wst.2012.334.

Zhao, B. et al., 2018. The Role of Reactive Iron in the Preservation of Terrestrial Organic Carbon in Estuarine Sediments. Journal of Geophysical Research: Biogeosciences, 123(12): 3556-3569, https://doi.org/10.1029/2018jg004649.

939 Zhao, Q. et al., 2016. Iron-bound organic carbon in forest soils: quantification and
940 characterization. Biogeosciences, 13(16): 4777-4788,
941 https://doi.org/10.5194/bg-13-4777-2016.
942

Supplementary Information

Mass balance calculation

To account for the mass loss during the extraction experiment we applied the mass balance calculation of Salvadó et al. (2015) combined with Peter and Sobek (2018). The %OC loss is calculated by applying bulk %C to the pre extraction mass and post extraction %C to the final mass. Comparison by change in raw %C is likely to overestimate the final %C if start and end carbon concentrations are calibrated to the initial mass, as when %C reduces so does the sample mass. Supplementary Equation 1 was devised to determine %OC-Fe loss.

Supplementary Equation 1

$$\Delta C(\%) = \frac{\left(M^{Pre(R)} x\ \%C^{Bulk}\right) - \left(M^{Post(R)} x\ \%C^{Post(R)}\right)}{M^{Pre\ (R)} x\ \%C^{Bulk}} - \frac{\left(M^{Pre(C)} x\ \%C^{Bulk}\right) - \left(M^{Post(C)} x\ \%C^{Post(C)}\right)}{M^{Pre\ (C)} x\ \%C^{Bulk}} \times 100$$

$M^{Pre/Post(R/C)}$ = Mass pre/post (R) reduction / (C) control.

$\%C^{Post(R/C)}$ = %C Post reduction/control experiment.

$\%C^{Bulk}$ = %C in the sediment pre extraction (same for control and reduction).

X-Ray Diffraction Analysis

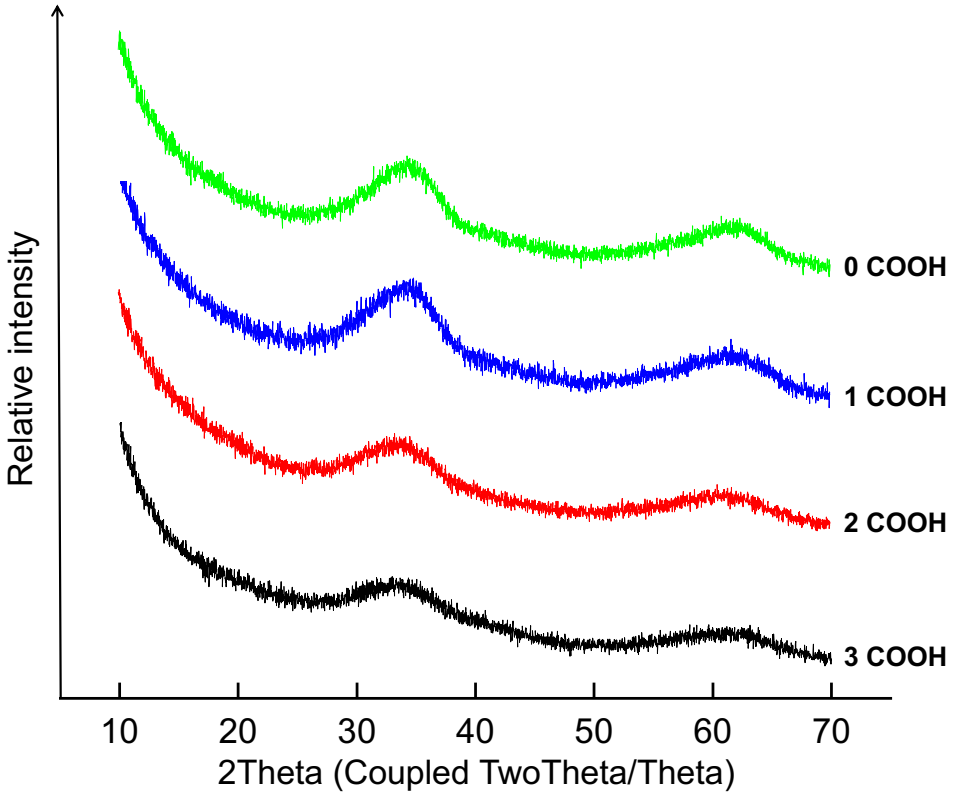

Figure S.1- Stacked XRD of coprecipitates with increasing carboxyl rich organic content.

Statistical Analysis

Ordinary one-way ANOVA

A one-way ANOVA test was conducted for %OC-Fe extraction values (Figure 2) and %Fe extraction values (shown in Figure 4) across the carboxyl range. The one-way ANOVA was applied to these two data sets as a comparative measure of sample means across the groups. The one-way ANOVA is limited by only having the ability to report whether there is a difference in means between two groups. Hence, a Tukey honest significant difference (HSD) test was applied post-hoc to determine the exact groups for which a statistically significant difference in means occurred for at the 99% significance level (**Table S1 and S2).** All analyses were conducted in GraphPad Prism version 8.30, GraphPad Software, La Jolla California USA, www.graphpad.com.

Table S1: Tukey's multiple comparisons test of extracted %OC-Fe for carboxyl coprecipitates.

Comparison	Adjusted P Value	Significant?*
1 COOH vs 2 COOH	<0.0001	Yes
1 COOH vs 3 COOH	<0.0001	Yes
2 COOH vs 3 COOH	0.0001	Yes

*Significance was determined at the 99% significance level.

Table S2- Tukey's multiple comparisons test of extracted %Fe for carboxyl coprecipitates.

Comparison	Adjusted P Value	Significant?*
0 COOH vs 1 COOH	0.0050	Yes
0 COOH vs 2 COOH	<0.0001	Yes
0 COOH vs 3 COOH	<0.0001	Yes
1 COOH vs 2 COOH	<0.0001	Yes
1 COOH vs 3 COOH	<0.0001	Yes
2 COOH vs 3 COOH	0.0019	Yes

*Significance was determined at the 99% significance level.

Determination of %OC-Fe

Table S3 shows the raw data for the reduction and control stages of the CBD treatment which were used as inputs to Equation 1 in order to calculate %OC-Fe as shown in Figures 2 and 3

Table S3- Raw carbon data for determining %OC-Fe.

wt %OC-Fe in sample	Bulk %OC*	Reduction (Δ %OC)	Control (Δ %OC)	%OC-Fe extracted
		1 COOH		
20	0.636	-12.527 (± 21.056)	78.606 (± 11.716)	-91.132 (± 9.340)
30	0.968	17.398 (± 7.741)	95.968 (± 1.162)	-65.189 (± 9.346)
40	0.978	-19.607 (± 2.243)	87.622 (± 9.317)	-107.229 (± 11.560)
50	1.357	10.854 (± 9.315)	92.742 (± 4.386)	-81.888 (± 13.702)
		2 COOH		
20	1.681	74.066 (± 5.818)	75.944 (± 1.457)	-1.879 (± 7.275)
30	2.192	71.080 (± 2.150)	70.613 (± 9.976)	0.467 (± 12.126)
40	3.237	63.203 (± 8.030)	78.079 (± 2.245)	-14.876 (± 10.275)
50	3.639	70.423 (± 1.234)	77.892 (± 2.123)	-7.468 (± 3.357)
		3 COOH		
20	2.761	87.043 (± 3.224)	46.620 (± 4.390)	40.423 (± 7.615)
30	4.339	91.764 (± 1.881)	44.503 (± 3.625)	47.260 (± 5.506)
40	5.420	91.628 (± 0.686)	41.114 (± 0.629)	50.514 (± 1.315)
50	6.935	89.602 (± 0.487)	43.036 (± 0.485)	46.566 (± 0.973)

*Bulk %OC refers to the OC content prior to any treatment. Values shown are a mean of duplicates, ± indicates the standard error of the mean (SEM).

References:

Salvadó, J.A. et al., 2015. Organic carbon remobilized from thawing permafrost is resequestered by reactive iron on the Eurasian Arctic Shelf. Geophysical Research Letters, 42(19): 8122-8130, https://doi.org/10.1002/2015gl066058.

Peter, S., Sobek, S., 2018. High variability in iron-bound organic carbon among five boreal lake sediments. Biogeochemistry, 139(1): 19-29, https://doi.org/10.1007/s10533-018-0456-8.